Progress In Electromagnetics Research M, Vol. 95, 115–123, 2020

Amplitude Steerable Antenna Based on Reconfigurable Ratio Power Divider

Iyemeh Uchendu[1, *] and James Kelly[2]

Abstract—This paper presents a highly innovative approach of amplitude steering without the use of variable gain amplifiers (VGA). This approach involves the use of a Reconfigurable Ratio Power Divider (RRPD) and does not suffer from the instability, poor efficiency, and worsened SNR associated with the use of VGAs. The RRPD, which is reconfigured manually by means of a potentiometer, is used to feed a 2×1 antenna array. By varying the power dividing ratio of the RRPD, continuous beam steering is achieved through passive amplitude control. The antenna was designed to operate at 2.4 GHz and had a continuous steering range from 0° to 21° while maintaining a stable return loss around the centre frequency. An expression that relates the reconfigurable ratio to the variable resistance was derived empirically. The prototype amplitude steerable antenna was fabricated and measured to validate the analyses.

1. INTRODUCTION

Beam steerable antennas have found applications in many aspects of radio wave communication and radar technology. Antennas with beam steering capabilities have the ability to reconfigure the main beam of their radiation pattern towards a desired direction to improve the strength of a desired signal whilst reducing the strength of undesired signals (or interference) originating from other directions. Several techniques such as phased arrays, parasitics, integrated lens antennas, reflectarrays, metamaterial antenna and switched beam antennas have been used to implement beam steering [1].

Amplitude steering is another technique used to achieve beam steering. It involves altering the amplitude of the signals fed to the driven element in order to reconfigure the radiation pattern of the antenna. The approach is similar in concept to taking the resultant of several vectors; one vector for each radiating element in the array. The amplitude of the signal applied to each element is equivalent to the magnitude of the vector and the direction of the main beam from each element is equivalent to the phase of the vector. By changing only the magnitude of two vectors, the phase of the resultant between the two vectors can be altered. This concept was introduced in [2] with the aim of reducing the number of phase shifters and delay lines used in a phased array antenna. The conventional approach for altering the amplitude of the signals fed to the driven elements is to employ Variable Gain Amplifiers (VGAs). The authors made use of VGAs and a 90° phase shift delay line to implement amplitude steering. This approach offers continuous beam steering when the amplitudes of the weights are continuously varied. A major drawback of the design, reported in [2], is that the antenna develops a secondary beam which is equal in gain to the main lobe. Unfortunately, it is then necessary to implement a technique to reduce the amplitude of the secondary beam, which is complex. Based on the design in [2], the authors of [3] presented detail analyses and equation that relate the steering resolution of the design to the amplitude of the signal fed to each radiating element. In [4], the authors used VGAs to achieve beam steering by altering the amplitude of the signals fed to each of the array elements. The authors designed a printed

Received 16 June 2020, Accepted 6 August 2020, Scheduled 16 August 2020
* Corresponding author: Iyemeh Uchendu (iyemehuchendu@unical.edu.ng).
[1] University of Calabar, Nigeria. [2] Queen Mary University, London, UK.

discrete lens array where 2 radiating elements were placed at the focal point on the feed side of the lens. A continuous beam steering range of $\pm 30^{\circ}$ was achieved. However, due to the non-uniform illumination loss, spill-over loss, mismatch loss, and ohmic loss within the lens, the gain of the antenna in the receive mode was significantly deteriorated.

The target of other reported work that made use of amplitude control was to achieve beam shaping and side lobe reduction [5–7]. Amplitude steering using VGAs is not commonly employed in practice due to: 1) behavioural instability in actively loaded antennas, as noted in the experiments reported in [8]; 2) the noise performance of the amplifier which reduces the total signal to noise ratio (SNR) of the system [9]; 3) reduction in efficiency and gain during beam steering; and 4) the biasing circuitry of the amplifier that may have a negative effect on the radiation pattern of the antenna. In order to combat these limitations, this paper presents a novel approach for implementing amplitude steering using a reconfigurable ratio power divider (RRPD). The designed RRPD is a passive, manually controlled component which avoids: 1) the behavioural instability in actively loaded antennas, 2) does not contribute to the SNR of the system, 3) maintains the power supplied to the antenna by rerouting power from one port to the other, and 4) preserves the radiation pattern of the antenna.

This paper is structured as follows: Section 2 presents details relating to the design and fabrication of the proof-of-concept amplitude steerable antenna incorporating an RRPD. Section 3 presents the results and discussion. Section 4 presents the conclusions.

2. RRPD AND ANTENNA DESIGN

Figure 1 shows the structure of the proposed RRPD which is based on the conventional Wilkinson unequal power divider where the isolating resistor is replaced with a potentiometer. A compensated impedance (Z_1) is introduced into the RRPD structure to allow more control over the impedance of the dividing arms. The equation relating the compensated impedance to the impedance of the dividing arms is given below:

$$Z_2 = Z_1\sqrt{\frac{2}{k^2}} \tag{1}$$

$$Z_3 = k^2 Z_2 \tag{2}$$

where k^2 is the designed ratio of the power divider; Z_1 is the compensated impedance; Z_2 is the impedance of the high power arm; and Z_3 is the impedance of the low power arm.

The variable resistance (R_{var}) in Fig. 1 is critical to achieving ratio reconfiguration. When R_{var} is set to its minimum value of $0\,\Omega$, the potential difference between the outputs of dividing arms will be $0\,\mathrm{V}$ (i.e., equivalent to a short circuit), hence the power in both arms will be the same. R_{var} sets the potential difference between the dividing arms thereby controlling the ratio of power division between the dividing arms. This is the main difference between the proposed design and the convention unequal Wilkinson unequal power divider. The new insight reported in this paper and utilised in our proposed design is that the isolating resistance in a conventional unequal power divider does not only improve the isolation between the output ports, but it can also be used to alter the power dividing ratio.

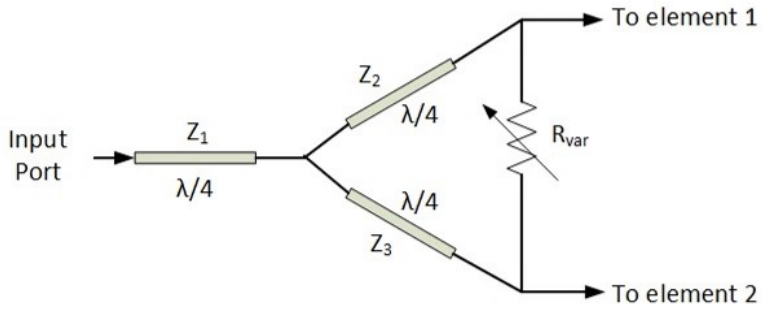

Figure 1. Structure of reconfigurable ratio power divider.

The relationship between the reconfigurable ratio and the variable resistance of the proposed RRPD was obtained through empirical study and is presented in the equation below.

$$Y = \frac{2(a^2-1)}{\pi}\tan^{-1}\left(\frac{0.45\pi}{180a}R_{var}\right)+1 \tag{3}$$

where Y is the reconfigurable ratio (i.e., the ratio of S_{21} to S_{31}); a is the designed ratio of the unequal divider (k^2); and R_{var} is the variable resistance. Three prototypes of the proposed RRPD with ratios of $1:1.5$, $1:2.0$, and $1:2.5$ were designed and analysed using ADS. For each prototype, R_{var} was varied from 0–20 kΩ in steps of 100 Ω, and the ratio of S_{21} to S_{31} was obtained, at the operating frequency. Fig. 2 shows the relationship between the ratio of S_{21} to S_{31} and the value of R_{var}. The values obtained using Eq. (3) are also plotted in Fig. 2. There is excellent agreement between the two curves, shown in Fig. 2, thus validating Eq. (3).

From the analyses, it can be seen that the reconfigurable ratio (Y) of the divider has a range of ratios which starts from 1, when $R_{var} = 0$ and approaches the square of the designed dividing ratio (k^2) when R_{var} approaches infinity. Hence for the $1:1.5$, $1:2.0$, and $1:2.5$ prototypes, Y has a range of 1–2.25, 1–4.00 and 1–6.25 respectively.

For a proof-of-concept solution, a standard low frequency film type (CERMET) potentiometer was used to implement R_{var}. An equivalent circuit for a film type potentiometer was unavailable at the time of writing. In order to model the behaviour of the potentiometer in ADS, an equivalent circuit for a flm type resistor was used [10] with the reistance replaced by a variable resistance. This approach was justified since the film type resistor had a similar package to the potentiometer. Fig. 3 shows an approximate equivalent circuit of the potentiometer. However, this circuit has not be experimentally validated.

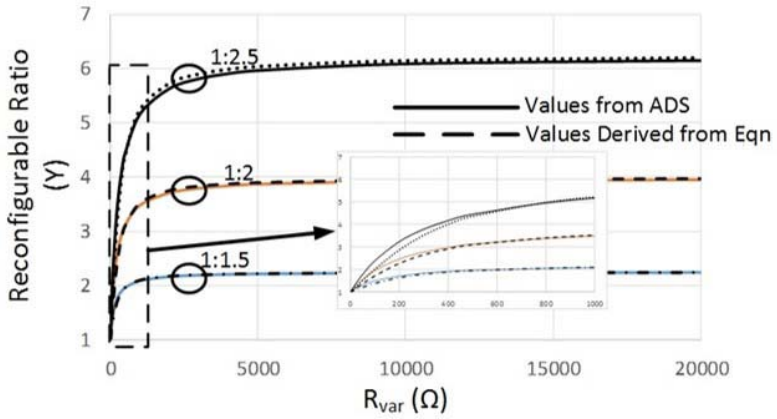

Figure 2. Relationship between reconfigurable ratio (Y) and R_{var}.

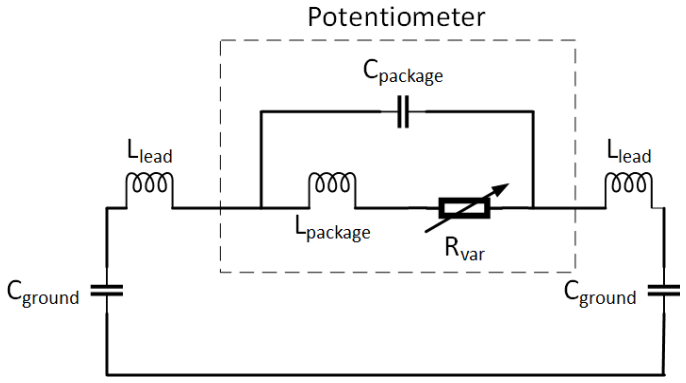

Figure 3. Approximate equivalent circuit of a film type potentiometer.

The reactances in the potentiometer are: 1) the inductance of the wiper arm (L_{package}), 2) capacitance between the packaging and the resistive element (C_{package}), 3) the inductance developed in the connecting leads (i.e., the terminals of the component) (L_{lead}), and 4) the capacitance between the body of the lumped element and the ground (C_{ground}).

The next step was to connect the output of the RRPD to a 2×1 antenna array. The effect of changing the power dividing ratio, of the RRPD, on the surface current density of the array antenna was studied. Fig. 4 shows the surface current distribution for various power dividing ratios between the array elements. When the power dividing ratio is $1:1$, the surface current density shown in Fig. 4(a), is obtained. The resulting radiation pattern features a main beam directed towards boresight. When the power dividing ratio is: $2:1, 3:1$, and $4:1$, the surface current distribution on the antenna changes. The corresponding surface current distributions are shown in Figs. 4(b)–(d). This use of an unequal power division ratio has the effect of steering the main beam of the antenna steering towards the element with a lower surface current density. By changing the dividing ratio, the amplitude of the signal fed to each element is altered, hence resulting in amplitude steering. For a proof-of-concept solution, a potentiometer was used to implement the variable resistance.

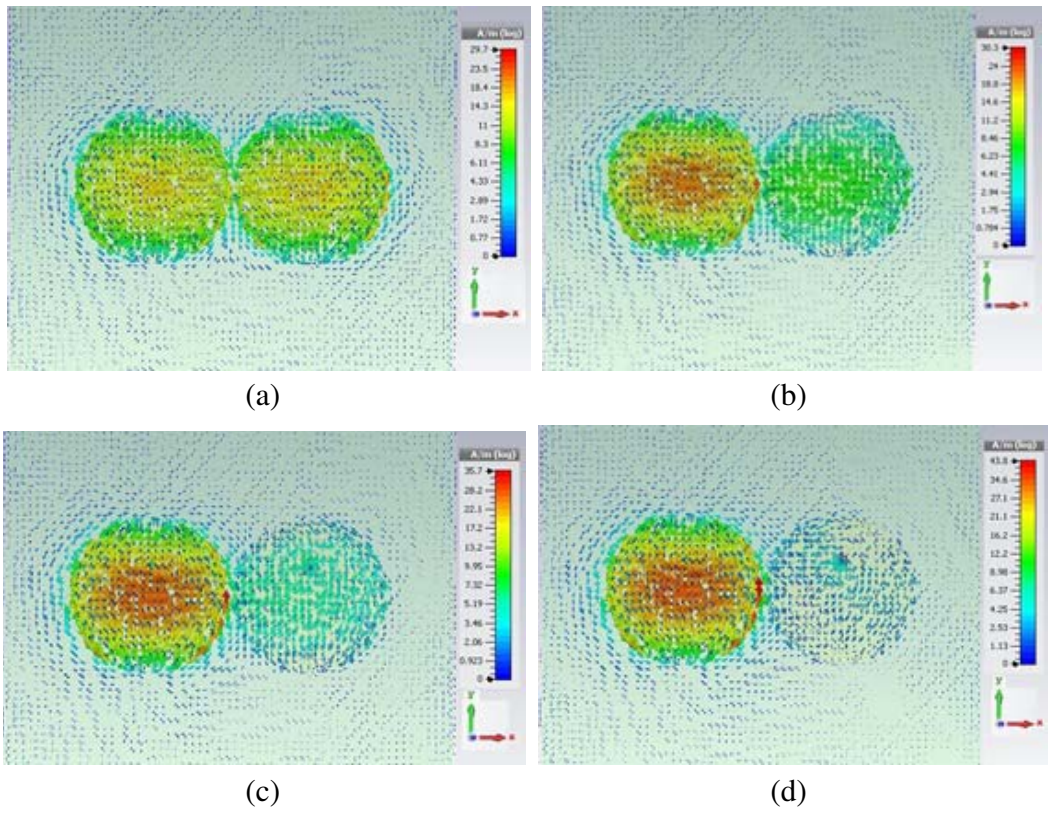

Figure 4. Surface current distribution at 2.4 GHz. (a) Ratio $1:1$, (b) Ratio $2:1$, (c) Ratio $3:1$, (d) Ratio $4:1$.

This gives a manual means of reconfiguring the ratio of the RRPD and in turn, of steering the main beam of the array antenna. The potentiometer also offer a continuous means of reconfiguring the RRPD, which in turn offers a continuous beam steering capability. The potentiometer was modelled in ADS using a lumped element equivalent circuit consisting of a series resistance and inductance in parallel with a capacitance. Changing the value of the resistance, at RF altered the impedance of the potentiometer and hence the dividing ratio of the RRPD, at the operating frequency. Hence, in this work, the potentiometer is used as a variable impedance to prove the concept of amplitude steering using the RRPD.

3. RESULTS AND DISCUSSION

Figure 5 shows the layout and dimensions of the designed RRPD. The RRPD was designed with an unequal ratio of 1 : 2.5 (i.e., $k^2 = 2.5$) to operate at a frequency of 2.4 GHz. The compensated impedance (Z_1) was set to 60 Ω in order to reduce the width of the high power impedance arm (Z_2). Z_2 and Z_3 were calculated, using Eqs. (1) and (2), to be 53.67 Ω and 134.16 Ω respectively. The substrate used was FR4 with dielectric constant of 4.55, thickness of 1.6 mm, and loss tangent of 0.0175, at 1 MHz. These values were obtained from the manufacturers datasheet. A BOURNS 3386 potentiometer having a value of 1 kΩ was used as the variable resistance.

The antenna array comprised two circular microstrip elements each with radius of 16.8 mm and had an interelement spacing of $0.53\lambda_g$ centre-to-centre. The feed point of the driven elements was 6.25 mm above the centre of the patch along the y-axis. The antenna was fabricated on the same substrate as the RRPD. The RRPD and the antenna were designed to fit back-to-back. Fig. 6 shows the fabricated antenna and RRPD. The maximum value of the potentiometer is referred to as Max. Z while the minimum value is Min. Z.

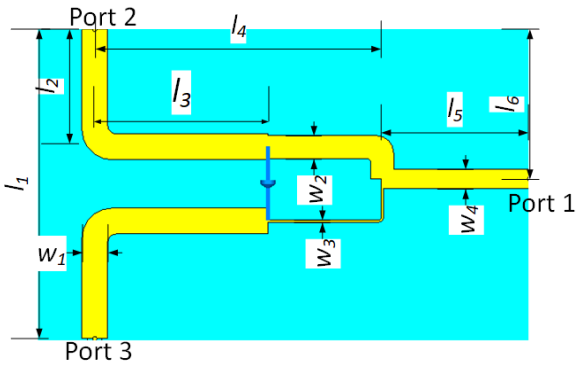

Figure 5. Layout of designed RRPD (l_1 = 35.6 mm; l_2 = 13.55 mm; l_3 = 20 mm; l_4 = 32.2 mm; l_5 = 17.02 mm; l_6 = 17.22 mm; w_1 = 2.96 mm; w_2 = 2.62 mm; w_3 = 0.24 mm; w_4 = 2.14 mm).

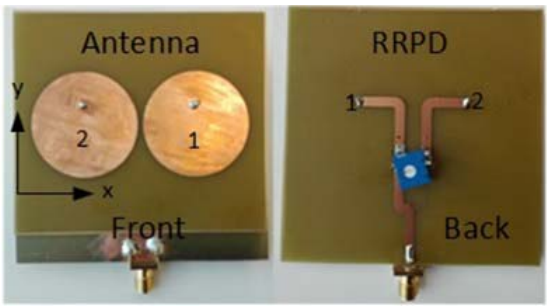

Figure 6. Fabricated prototype of proof-of-concept antenna and RRPD.

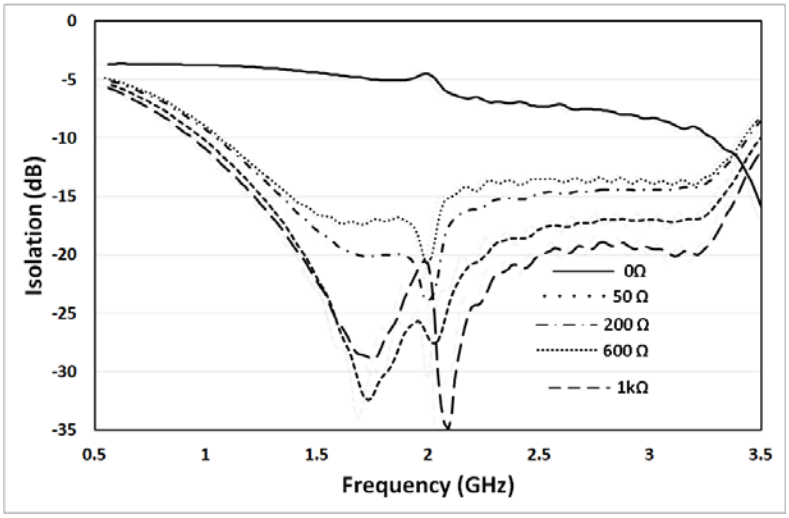

Figure 7. Isolation between the output ports for different potentiometer settings.

Before connecting the antenna to the RRPD, we attached connectors to the output ports to measure the isolation between the ports as R_{var} changes. Fig. 7 shows the isolation between the ports for five different values of the potentiometer before installation. At 0 Ω, the isolation between the ports is poor, which is expected as it would mean shorting the output terminals to each other. The isolation improves as the value of R_{var} increases. This shows that the ports are well isolated and there is no coupling between the ports.

Figure 8 shows the return loss of the combined antenna array and RRPD.

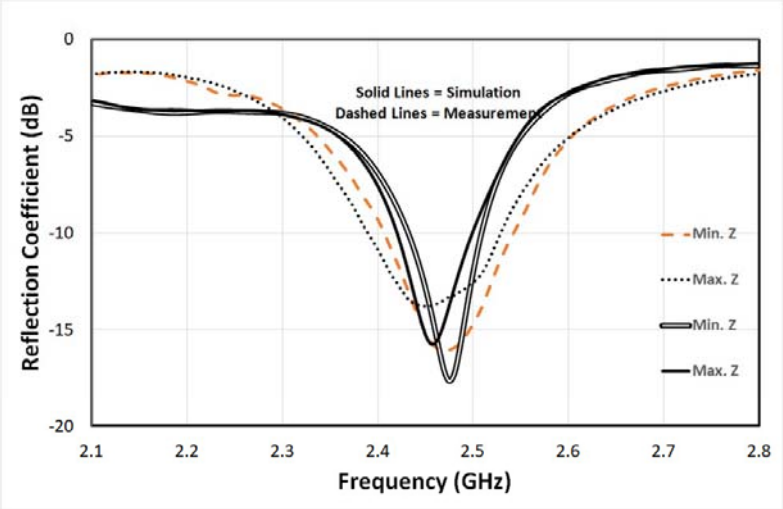

Figure 8. Return loss of amplitude steering antenna.

The return loss zeros for the antenna lie at 2.46 GHz (for Max. Z) and 2.48 GHz (for Min. Z), which shows that altering the potentiometer has little effect on the operating frequency. The return loss for Min. Z is better than 15 dB, but as the power dividing ratio increases, the return loss degrades slightly. The worst-case return loss, i.e., Max. Z is better than 13 dB. The measured return loss shows a wider bandwidth when compared to simulation. This could be attributed to the difference between the modelled values of the potentiometer impedance and the actual values of potentiometer impedance.

Figure 9 shows the E-plane radiation pattern of the antenna when the potentiometer is set to the Min. Z value, which corresponds to an equal power dividing ratio. The main beam of the antenna, in this situation, is directed towards boresight and the surface current density, on the two driven elements,

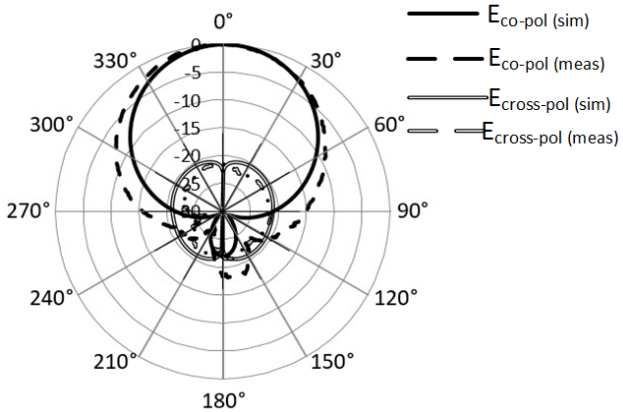

Figure 9. Radiation pattern for equal power dividing ratio (Min. Z) between the array elements.

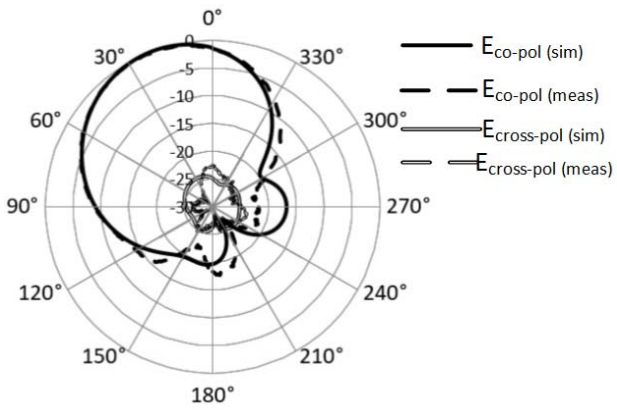

Figure 10. Radiation pattern for maximum power dividing ratio (Max. Z) between the array elements.

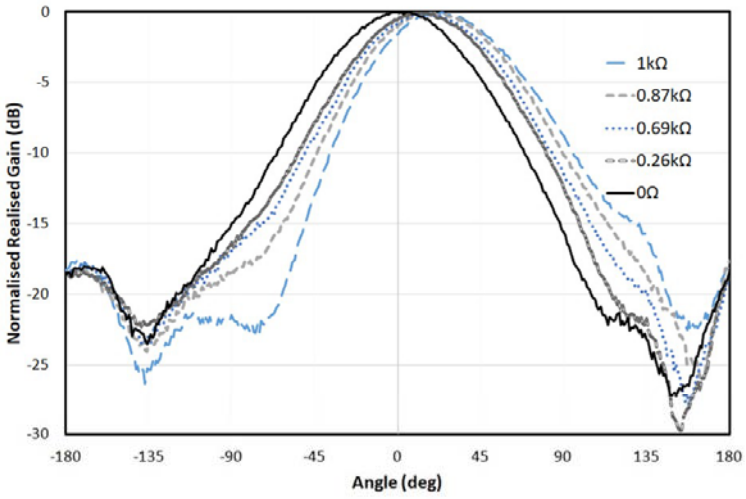

Figure 11. Radiation pattern showing various steering angles for different intermediate potentiometer settings.

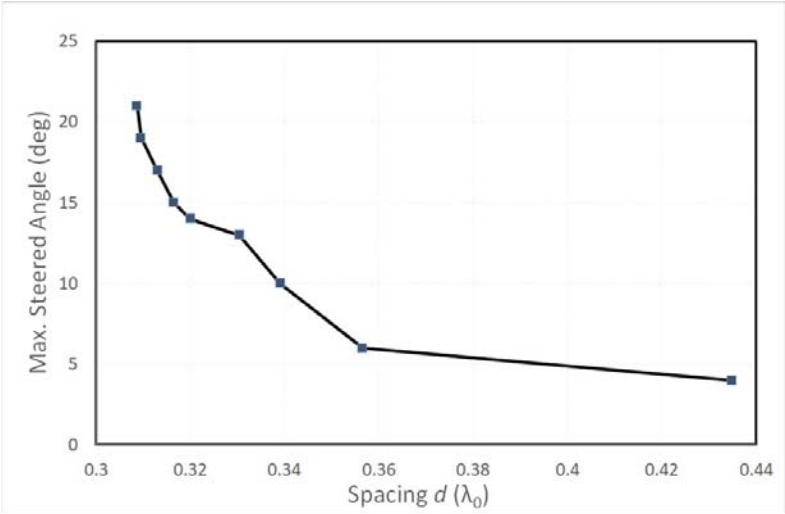

Figure 12. Max. steered angle vs. centre-to-centre spacing.

is equal. The antenna has a realised gain of 5.2 dB for this potentiometer setting.

By increasing the value of the potentiometer, the main beam of the antenna array is steered towards the direction of the element with the lower surface current density, which is element 2 based on Fig. 6. Fig. 10 shows the E-plane radiation pattern of the antenna when the potentiometer is set to a value of Max. Z. The antenna has a realised gain of 4.1 dB and main beam steering angle of 21° for this potentiometer setting. This corresponds to the maximum steering range of the antenna. For all potentiometer settings the E-plane cross-polar radiation patterns of the antenna are more than 20 dB lower than the E-plane co-polar radiation patterns. The resistance of the potentiometer was measured at several different rotational settings before installation into the circuit. At these settings, the potentiometer had the following values: 0.26 kΩ, 0.69 kΩ, and 0.87 kΩ. Fig. 11 shows the measured radiation patterns corresponding to these settings. The scan loss of the antenna as it steers towards the maximum direction is approximately 0.05 dB/deg. The scan loss for a conventional phased array incorporating ideal (lossless) phase shifters is estimated to be 0.02 dB/deg. This estimate was obtained assuming a scan loss of $\cos\theta$, where θ = the main beam steering angle [11]. Hence, the scan loss of the proposed an amplitude steerable antenna will be lower than that of a conventional phased array when

real phase shifters are used due to the high losses incurred in the phase shifters.

The total efficiency of the antenna varies from 55% (for Min. Z) to about 45% (for Max. Z). Upon re-running the simulation with a lossless dielectric substrate, the worst-case efficiency (i.e., for a potentiometer setting of Max. Z) was found to be 81%. This indicates that dielectric losses, within the substrate are a major contributor to the poor efficiency values, reported above. The insertion losses within the RRPD, due to the parasitic effects within the potentiometer, are likely to partly account for the remaining loss of efficiency.

To study the effect of the inter-element spacing between the radiating elements on the overall radiation pattern of the antenna, a number of simulations were performed in which the centre-to-centre spacing between the radiating elements was varied. Fig. 12 shows the maximum steered angle corresponding to each value of centre-to-centre spacing. It is clear that the maximum steered angle reduces as the spacing between the elements increase. This behaviour is similar to that of a conventional phased array antenna.

4. CONCLUSION

The concept of beam steering by controlling the amplitude of the signals fed to the radiating elements of a phased array has been known since 1976; however, it is not commonly used due to the drawbacks in using Variable Gain Amplifiers. These drawbacks are: 1) behavioural instability in actively loaded antennas, 2) degradation of the systems SNR due to the noise figure of the VGA, 3) reduction in efficiency and gain during beam steering, and 4) effect of the biasing circuitry on the radiation pattern of the antenna.

This paper presents a novel approach for achieving amplitude steering by using a Reconfigurable Ratio Power Divider (RRPD) instead of VGAs. By making use of the RRPD the following were achieved: 1) the antenna performance was stable as the amplitude control is passive; 2) better system performance as the RRPD does not contribute as much noise when compared with amplifiers to the SNR; 3) A fairly stable gain and efficiency, as a function of main beam steering angle, because the RRPD re-routes the power supplied between the driven element while keeping the total power supplied to the antenna array constant; and 4) the radiation pattern of the antenna is preserved as the RRPD is operated manually by the use of a potentiometer. The amplitude steerable antenna can steer the beam from 0° to 21° towards one direction. A proof-of-concept antenna was fabricated and measured to validate the analyses. The measurement results show good agreement with simulations.

ACKNOWLEDGMENT

The authors would like to acknowledge the financial support of EPSRC (EP/P008402/1) which help to facilitate the prototype fabrication and measurement. We would also like to thank the Nigerian Information Development Agency (NITDA) for funding the first authors PhD scholarship.

REFERENCES

1. Uchendu, I. and J. R. Kelly, "Survey of beam steering techniques available for millimeter wave applications," *Progress In Electromagnetics Research B*, Vol. 68, 35–54, 2016.
2. Hughes, W. J. and W. Thompson, "Tilted directional response patterns formed by amplitude weighting and a single 90° phase shift," *Journal of the Acoustical Society of America*, Vol. 59, 1040, 1976.
3. Fraizer, C. H., W. J. Hughes, and W. D. O'Brain, "Analyses of resolution for an amplitude steered array," *Journal of the Acoustical Society of America*, Vol. 107, 2430, 2000.
4. Rondineau, S., S. Romisch, D. Popovic, and Z. Popovic, "Multibeam spatially-fed antenna arrays with amplitude-controlled beam steering," *2003 27th Antenna Applications Symposium*, 25–37, Moticello, Illinois, 2003.

5. Copeland, J., W. Robertson, and R. Verstraete, "Antennafier arrays," *IEEE Trans. Antennas and Propag.*, Vol. 12, No. 2, 227–233, 1964.
6. Mielke, W., "An active phase shifter for phased array applications providing amplitude and phase control," *1985 15th European Microwave Conference*, 572–577, Paris, France, 1985.
7. Rabinovich, V. and N. Alexandrov, *Antenna Arrays and Automotive Applications*, Springer, New York, 2013.
8. Fanson, P. L. and K. Chen, "Instabilities and resonances of actively and passively loaded antennas," *IEEE Trans. on Antennas and Propag.*, Vol. 6, 344–347, 1974.
9. Fujimoto, K., "On the noise performance of amplifier-antenna systems," *Proceedings of the IEEE*, Vol. 53, No. 10, 1671–1672, Oct. 1965.
10. Beyschlag, V., "Resistors in microwave applications," *Appl. Note 28871*, 1–6, 2013.
11. Ho, T. Q., C. A. Hewett, L. N. Hunt, T. G. Ready, and R. Mittra, "Lattice spacing effect on scan loss for bat-wing phased array antennas," *2005 IEEE/ACES Int. Conf. Wirel. Commun. Appl. Comput. Electromagn.*, 245–248, 2005.